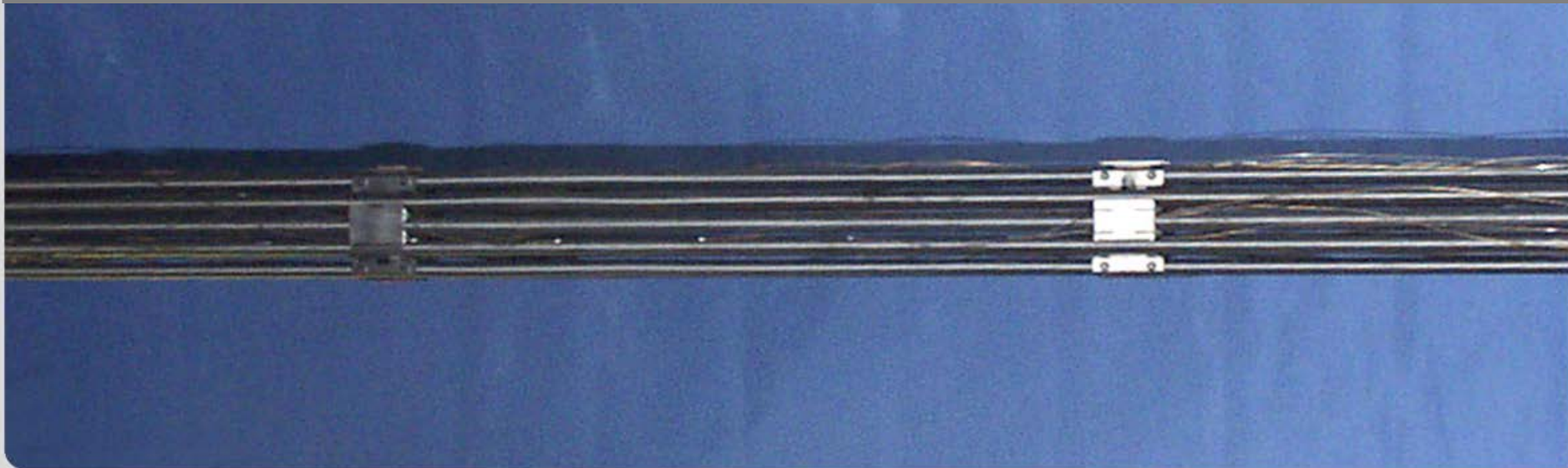


Modeling of QUENCH bundle tests using ASTEC v2.0p2 -towards new benchmark activities at KIT-

H. Muscher

18th International QUENCH Workshop, Karlsruhe, 20.-22. Nov. 2012

Institute for Applied Materials
Materials Process Technology, Programme NUKLEAR



QUENCH test matrix



Test	Quench medium / Injection rate	Temp. at onset of flooding	Max. ZrO ₂ before transient	Max. ZrO ₂ before flooding	Max. ZrO ₂ after test	H ₂ production before / during cooldown	Remarks, objectives
QUENCH-00 Oct. 9 - 16, 97	Water 80 g/s	≈ 1800 K			completely oxidized		commissioning test
QUENCH-01 February 26, 98	Water 52 g/s	≈ 1830 K	312 μm		500 μm at 913 mm	36 / 3	pre-oxidized cladding
QUENCH-02 July 7, 98	Water 47 g/s	≈ 2400 K			completely oxidized	20 / 140	COBE: no additional pre-oxidation
QUENCH-03 January 20, 99	Water 40 g/s	≈ 2350 K			completely oxidized	18 / 120	no additional pre-oxidation
QUENCH-04 June 30, 99	Steam 50 g/s	≈ 2160 K	82 μm		280 μm	10 / 2	slightly pre-oxidized cladding
QUENCH-05 March 29, 2000	Steam 48 g/s	≈ 2020 K	160 μm		420 μm	25 / 2	pre-oxidized cladding
QUENCH-06 Dec. 13 2000	Water 42 g/s	≈ 2060 K	207 μm	300 μm	670 μm	32 / 4	OECD-ISP 45
QUENCH-07 July 25, 2001	Steam 15 g/s	≈ 2100 K	230 μm		completely oxidized	66 / 120	COLOSS: B ₄ C
QUENCH-09 July 3, 2002	Steam 49 g/s	≈ 2100 K			completely oxidized	60 / 400	COLOSS: B ₄ C, steam starvation, very high T
QUENCH-08 July 24, 2003	Steam 15 g/s	≈ 2090 K	274 μm		completely oxidized	46 / 38	reference to QUENCH-07 (without B ₄ C)
QUENCH-10 July 21, 2004	Water 50 g/s	≈ 2200 K	514 μm	613 μm (at 850 mm)	completely oxidized	48 / 5	LACOMERA: air ingress
QUENCH-11 Dec 08, 2005	Water 18 g/s	≈ 2040 K		170 μm	completely oxidized	9 / 132	LACOMERA: boil-off
QUENCH-12 Sept 27, 2006	Water 48 g/s	≈ 2100 K	160 μm, breakaway	300 μm, breakaway	completely oxidized	34 / 24	ISTC: VVER
QUENCH-13 Nov. 7, 2007	Water 52 g/s	≈ 1820 K		400 μm	750 μm	42 / 1	SARNET: Ag/In/Cd (aerosol)
QUENCH-14 July 2, 2008	Water 41 g/s	≈ 2100 K	170 μm	470 μm	840 μm	34 / 6	M5 [®] cladding
QUENCH-15 May 27, 2009	Water 48 g/s	≈ 2100 K	145 μm	320 μm	630 μm	41 / 7	ZIRLO [™] cladding

Introduction/ Motivation/ Outline of the PSI- Benchmark Exercise

- ASTEC 2.0 rev.1 Modeling / CORA-13 – *at first*; Quench exp. sim. *followed*: level controlled by auxiliary feed water injection

→ Validation against exp. -code to data but still not code to code-

→ Training course at IRSN 1/2011, especially

ICARE which describes phenomena occurring in the degradation phase. Clad oxidation, rods heat up and melting etc.

➔ **QUENCH experiments provide data for development of models & codes:**

➔ App. of ASTEC on Quench problems/ comparing Zry-4, M5[®], E110

➔ At first only ICARE, ODESSA and MDB use

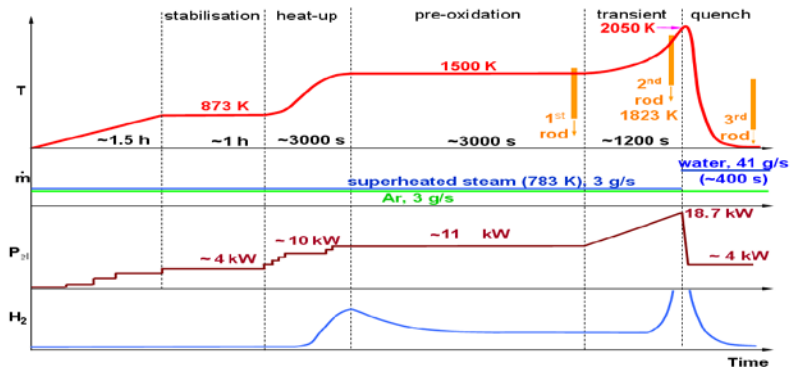
- BCs, Core degradation parameters/ Nominal s-s: given both by PSI and KIT

- The objectives /the scope of the BE -clearly outlined: radial and axial bundle profiles (power) according to **specification** as well as the Q-facility geometry

- **Chronology of main events-** given in a quick look table: FZKA reports



Time [s]	Event	Time [s]	Event
0	Start of data recording. Fuel bundle at 873 K (T1T A13), data acquisition frequency at 1 Hz. Oxidation starts: 3.5 g/y @ 775K.	0	Start data recording. T_{in} TFS 5/14=871 K, el. power switched from 4.3 to 9 kW. Start of pre-oxidation phase in gas mixture of overheated steam (Pm 205 = 3 g/s) and argon (Pm 4010 = 3 g/s).
521	Start of massup from 3.95 kW	(10:41:30h)	
2028	12.5 kW electric power reached. T1T A13: 1268 K	2291	Cl down switched from 9.8 to 18.8 kW. T_{in} TFS 6/13 = 1208 K.
2523	End of first transient. Temperature of F993(K;T1T A13) reached. End of electric power plateau at 12.5 kW	3002	El. power switched from 18.8 to 11.3 kW. T_{in} TFS 6/13 = 1300 K.
3710	First rod failure (No detection)	6301	Start of cooling phase. Reduction of el. power from 11.3 to 3.9 kW. T_{in} TFS 4/13 = 1428 K.
6919	End of pre-oxidation phase. Reduction of electrical power from 13.15 kW to 6.9 kW. T1T A13: 1056 K	(12:28:30h)	
10113	Heat rod failure (P411) (No detection)	7245	Corner rod B withdrawn
11283-11273	Withdrawal of corner rod B. T1T A13: 1193 K	7307	Start of air ingress phase. Turn on the air flow with flow rate 0.2 g/s. Switch of argon flow from 3 g/s to 1 g/s. Switch-off of steam supply (3 g/s at 7319 K). T_{in} TFS 6/14 = 958 K.
11332	Date acquisition frequency at 5 Hz	(12:43:22h)	
11526-11528	Start of air ingress. Reduction steam to 0 g/s	7321	First indication of air at mass spectrometer
11660	Target air flow 1.0 g/s reached	10276	Accelerated temperature increase at bundle elevation 9.050 mm. TCR 9 increased from 1445 to 1623 K.
12470	El. power increase from 6.9 kW to 7.3 kW	10400	
13000	El. power increase from 7.3 kW to 7.7 kW	12300	Accelerated temperature increase at bundle elevation 8.450 mm. TFS 4/8 increased from 1290 to 1700 K.
13120	El. power increase from 7.7 kW to 8.1 kW	13030	Transition to complete quench operation and to partial nitrogen consumption. Decrease of nitrogen flow rate through the orifice plate from 2.16 to 1.13 g/s.
13275	Withdrawal of corner rod D (TFS 5/9). T1T A13: 2085 K	10500 - 11120	Accelerated temperature increase at bundle elevation 7.250 mm. TCR 7 increased from 1255 to 1700 K.
13393	End of air ingress. Quench initiation	10567	Accelerated temperature increase at bundle elevation 6.250 mm. TFS 1/56 increased from 1118 to 1400 K.
13397	Should failure (P406; TSH 1201; TCI 120)	10567	First rod failure. No indication at mass spectrometer.
13404	Start of electric power reduction from 8.1 kW to 3.9 kW. T1T A13: 2116 K	10569	Corner rod D withdrawn
13407	Electric power at 3.9 kW (simulation of decay power)	11330	Initiation of fast water injection. Stop of overheated gas and argon supply (closing of the V 302 valve). Reaction of the T51 bundle with thermocouple.
13420	Rod failure (P411) (No detection)	11341	Initiation of fast water injection. Stop of overheated gas and argon supply (closing of the V 302 valve). Reaction of the T51 bundle with thermocouple.
13541	Water reached the orifice pipe (TFS 5/12 ending)	11390	Initiation of green water supply (Pm 104 increased from 0 to 53 g/s).
13712	Start of power shutoff	11413	Release of hydrogen and diborane
13713	Quench water shutoff (P 104)	11592	Should failure. Flow of argon from the annulus annulus into the bundle (Pm 408 increase).
13714	Electric power below 0.3 kW	11592	Should failure. Flow of argon from the annulus annulus into the bundle (Pm 408 increase).
13731	Quench water at zero	11395	Intensive water boiling in bundle (evaporation rate at 63 g/s). Indication by increased off-gas flow rate (P 601), constant collapsed water level at elevation 1.051 ± 0.20 mm.
13740	Date acquisition frequency at 1 Hz	11550	Constant evaporation rate at ~7 g/s (according to constant channel of 22.05 cm ²). Increase of collapsed water level at elevation L 501 = 570 mm to L 501 = 958 mm.
13779	End of data recording	11780	Thermocouple TFS 1317 and T 512 at bundle elevation 1350 mm melted with double-phase fluid. Collapsed water level at elevation 651 ± 1.70 mm.
		12047	Shutdown of the quench pump (Pm 104 decreased from 53 to 0 g/s).
		12089	Shutdown of electrical power supply (power reduction from 3.9 to 0 kW).
		14440	End of data recording. Stop of air flow into annulus. Bundle T_{in} TFS 10/12 = 990 K, around T_{in} TFS 10/10 = 492 K, L 501 = 920 mm. Total collapsed condensed water 380(2) g (around 0.175).
		(28:07:11)	L 501 = 854 mm – corresponding water mass inside bundle at 9590 g (measured after bundle dismantling). Water mass inside annulus: 7204 g.



Chronology of main events- a quick look table (BE Stage 1)

Time [s]	Event
0	Start of data recording, test bundle at 873 K (TIT A/13), data acquisition frequency at 1 Hz. Oxidation steam: 3.0 g/s @ 773 K
581	Start of heatup from 3.85 kW
2025	12.5 kW electric power reached. TIT A/13: 1285 K
2523	End of first transient. Temperature of 1593 K (TIT A/13) reached. End of electric power plateau at -12.5 kW.
3710	First rod failure (He detection)
9319	End of pre-oxidation phase. Reduction of electrical power from 13.15 kW to 6.9 kW. TIT A/13: 1695 K
10113	Next rod failure (P411; He detection)
11353-11373	Withdrawal of corner rod B. TIT A/13: 1193 K
11528	Data acquisition frequency at 5 Hz
11626-11628	Start of air ingress. Reduction steam to 0 g/s
11660	Target air flow 1.0 g/s reached
12470	El. power increase from 6.9 kW to 7.3 kW
13000	El. power increase from 7.3 kW to 7.7 kW
13125	El. power increase from 7.7 kW to 8.1 kW
13275	Withdrawal of corner rod D (TFS 5/9). TIT A/13: 2085 K
13393	End of air ingress. Quench initiation. TIT A/13: 2196 K; TSH 13/90 I: 2083 K
13397	Shroud failure (P 406, TSH 12/0 I, TCI 12/0)
13404	Start of electric power reduction from 8.1 kW to 3.9 kW. TIT A/13: 2116 K
13407	Electric power at 3.9 kW (simulation of decay power)
13429	Rod failures (P411; He detection)
13541	Water reached the off-gas pipe (TFS 512 wetting)
13712	Start of power shutoff
13713	Quench water shutoff (F 104)
13714	Electric power below 0.3 kW
13731	Quench water at zero
13740	Data acquisition frequency at 1 Hz
16079	End of data recording

Time [s]	Event
0 (10:41:35h)	Start data recording, $T_{max}=TFS\ 6/14=871\ K$, el. power switched from 4.3 to 9.7 kW. Start of pre-oxidation phase in gas mixture of overheated steam (Fm 205 = 3.4 g/s) and argon (Fm 401B = 3 g/s).
2291	El. power switched from 9.8 to 10.8 kW. $T_{max}=TFS\ 4/13=1306\ K$.
3002	El. power switched from 10.8 to 11.3 kW. $T_{max}=TFS\ 4/13=1360\ K$.
6301 (12:26:34h)	Start of cooling phase . Reduction of el. power from 11.3 to 3.9 kW. $T_{max}=TFS\ 4/13=1428\ K$.
7249	Corner rod B withdrawn.
7307 (12:43:22h)	Start of air ingress phase . Turn on the air flow with flow rate 0.2 g/s. Switch of argon flow from 3 g/s to 1 g/s. Switch-off of steam supply (0 g/s at 7319 s). $T_{max}=TFS\ 6/14=998\ K$.
7321	First indication of air at mass spectrometer.
10270... ...10400	Accelerated temperature increase at bundle elevation 9 (550 mm). TCR 9 increased from 1445 to 1620 K.
10300... ...10800	Accelerated temperature increase at bundle elevation 8 (450 mm). TFS 4/8 increased from 1290 to 1700 K.
10350... ...10650	Transition to complete oxygen starvation and to partial nitrogen consumption . Decrease of nitrogen flow rate through the off-gas pipe from 0.16 to 0.13 g/s.
10500... 11120	Accelerated temperature increase at bundle elevation 7 (350 mm). TCR 7 increased from 1205 to 1700 K.
10587	First rod failure: Kr indication at mass spectrometer.
10900... ...11341	Accelerated temperature increase at bundle elevation 6 (250 mm). TFS 15/6 increased from 1115 to 1400 K.
11330	Corner rod D withdrawn.
11341	Initiation of fast water injection. Stop of overheated gas and argon supply (closing of the V 302 valve). Reaction of the T511 bundle inlet thermocouple.
11350... 11413	Initiation of quench water supply (Fm 104 increased from 0 to 53 g/s).
11352... ...11560	<i>Release of hydrogen and nitrogen.</i>
11380	Shroud failure: flow of argon from the shroud annulus into the bundle (Fm 406 increase).
11395... ...11530	Intensive water boiling in bundle (evaporation rate ca. 53 g/s): indication by increased off-gas flow rate (F 601); constant collapsed water level at elevation L 501 = 530 mm.
11530... ...11780	Constant evaporation rate ca. 47.3 g/s (according to coolant channel of 33.65 cm ²). Increase of collapsed water level from elevation L 501 = 570 mm to L 501 = 995 mm.
11830	Thermocouples TFS 13/17 and T 512 at bundle elevation 1350 mm wetted with double-phase fluid. Collapsed water level at elevation L 501 = 1194 mm.
12047... ...12080	Shut down of the quench pump (Fm 104 decreased from 53 to 0 g/s).
14625	Shut down of electrical power supply (power reduction from 3.6 to 0 kW).
14640 (14:45:36h)	End of data recording. Stop of Ar flow into shroud annulus. Bundle $T_{max}=TFS\ 10/12=390\ K$; shroud $T_{max}=TSH\ 16/180=405\ K$, L 501 = 1020 mm. Total collected condensed water 33602 g (according to L 701).
(28.07.11)	L 501 = 654 mm – corresponding water mass inside bundle is 6590 g (measured after bundle dismounting). Water mass inside shroud annulus: 7264 g.

- contract between GRS and KIT on ASTEC usage signed 28.10.2010
- "Overview of the integral code ASTEC v2.0"
- "Evolution of ASTEC v2.0-rev1 with respect to the v2.0 source"
- **ASTEC** principles and **general modeling features**
- focus on the **ICARE** part within "ASTEC Training Course material"
- detailed ICARE user's manual; guidelines; **MARCUS** (web)
- At first: Understanding of "quench05.dat" input deck in the context of the KIT- QUENCH facility **real design** (TCs, etc)
- **best-estimate ASTEC-ICARE input deck** for Q tests : Q-10, **Q-13 Q-16: work is underway**: Stabilization/ Heat up/ Pre-ox/ Transient heat up/ Quenching
- activities: KIT Internal **Q-14** report published + available
- **Q-05 /-06 /-11 /-14** simulated with ASTEC V2.0 rev.1
- **QUENCH-10/-13/-16** to be further simulated
- Participation at GRS-IRSN; OECD TG- meetings / ERMSAR conference 2013 planned
- KIT-ASTEC **1.3** work done already 2006 by others (nodalization schemes, data fields, etc.
- Calc. on the Zry-4 cladding /steam interactions using SVECHA 2.0/10.0 performed – QWS 16
- hydrogenation in LORA



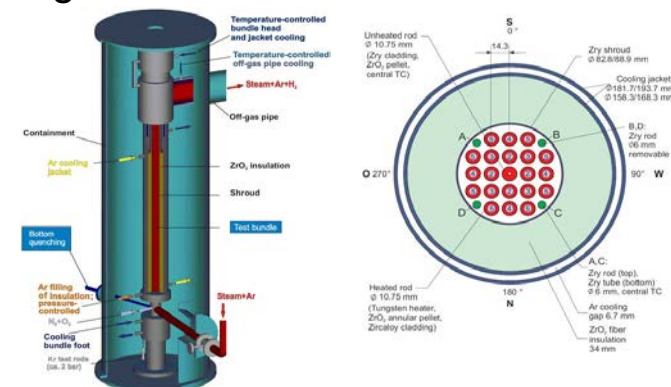
The aim is to present results of modeling **Q-5, Q-6, Q-11, Q-14, (later Q-10, Q-16, Q-13)** using ASTEC & test the applicability of ASTEC for modeling Q- experiments, which investigate the H₂ source term resulting from the water injection into an uncovered core as well as the high temp. behavior of core materials under transient conditions.

- Q-pre-test and post-test calculations done by others (using different tools, other experience..)
- App. of ASTEC to Q-experiments, code validation:
 - **Water quench:** Q-06 (ISP-45) Q-11 (Q-L2); **air ingress** Q-10/ Q-16
 - Assessment of core degradation/ delayed core reflood

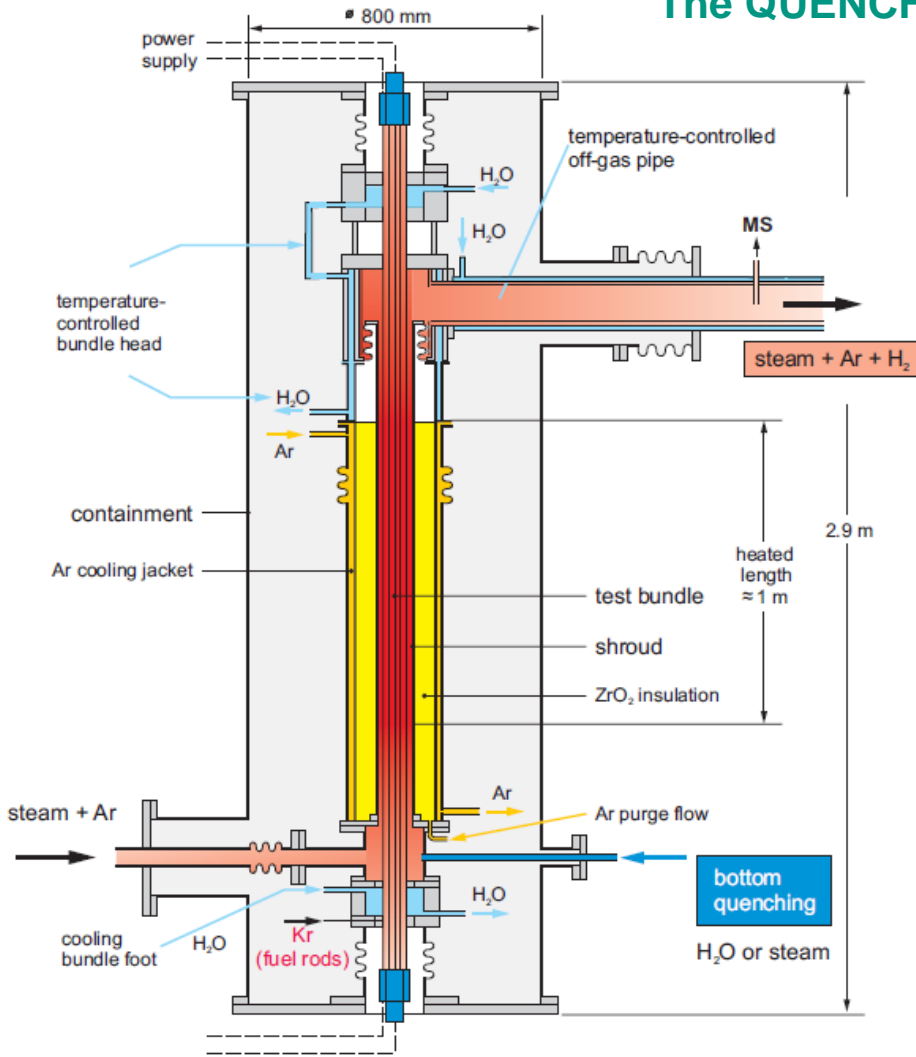
➤ Preparation of Q-10/ Q-16 IDs /SARNET Code BE: KIT the only one ASTEC participant so far ASTECv1.3 produced in former times somehow conflicting results because of an extrapolation of solid-state models to the processes in the liquid phase. The modeling of Zr-O **melt** oxidation, being independent of solid state processes, needs more consideration

→KIT ASTEC 1.3 IDs were rewritten, updated, for the purposes of the new ASTEC 2.0 rev2p2 (work done for **Q-06/Q-11/Q-14**): New IDs work in progress for Q-10; Q-16 Adopting 2D-MAGMA tool can lead to better results in simulating Q-tests than 1Dcandling.

- Revision according to new **BE specifications**
 - **CORE MESHING:** 6 radial fuel rings; 20 axial meshes
 - Inconel grids added
 - Apart of this,
- Q-13 v2.0. ID will be created based on optimized Q-11 ID.



The QUENCH-14 experiment



Q- Test section/ Modeling

- axial meshes, representative simulated fuel rods
- standard and improved Ar/O₂ ox kinetics

Superheated steam from the SG and super heater together with Ar enter test bundle at the bottom. Ar, steam and H₂ produced flow upwards inside the bundle and from the outlet at the top through a water-cooled off-gas pipe to the condenser, where the remaining steam is separated from the non-condensable gases Ar and H₂.

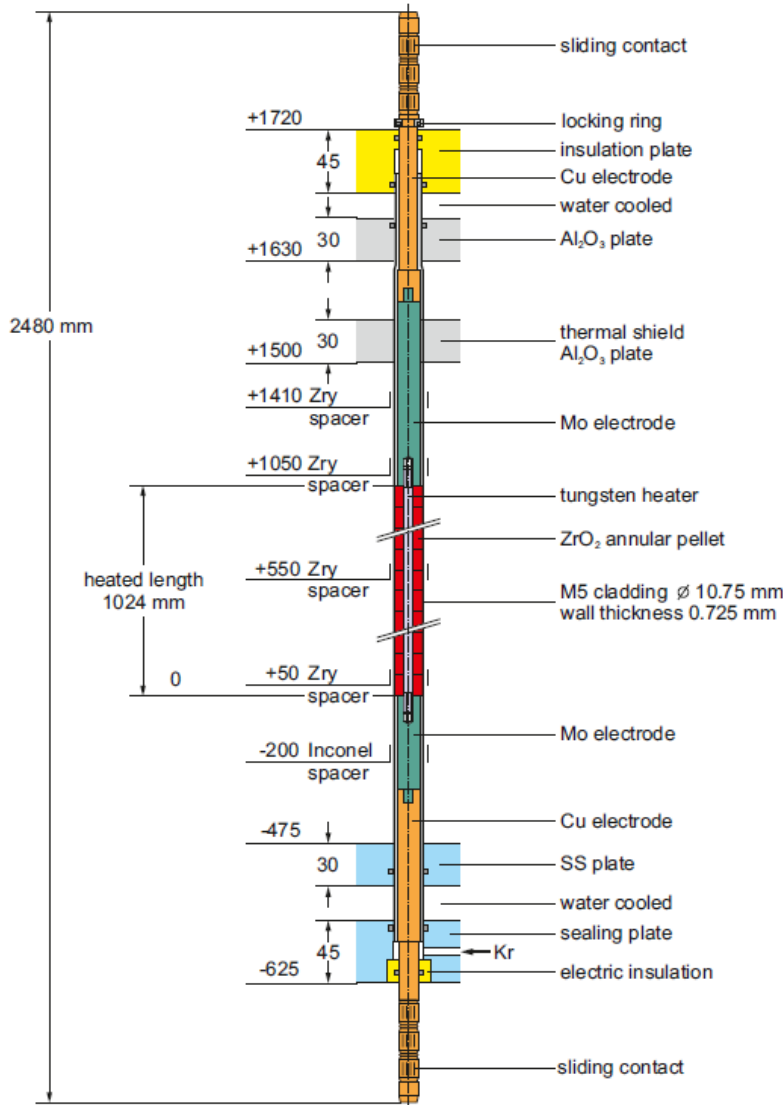
Facility:

- 21-rod type bundle, spacer grids
- rods el. heated with W bars (heated length: ca 1m)
- one central rod not heated used for instrumentation
- cladding: Zry, with annular pellets placed between W rods and the cladding itself
- air injection at the bottom part of the bundle

Test description (differs):

- pre-ox phase at >900°C by injection of Ar+25 % O₂ gas mix aiming at creating a ca 50 μm oxide layer
- air ingress phase init. at 900°C max temp. with injection of room temp. air and power kept const
- termination of the test foreseen at 2100°C max cladding temp by rapid cooling in a high flow of Ar at room temp with power switched off

The Q-14 experiment



Fuel rod simulator

Test bundle made of 21 fuel rod simulators and of 4 corner rods, held in their positions by 5 grid spacers, 4 of Zry-4, and one of Inconel 718 in the lower bundle zone.

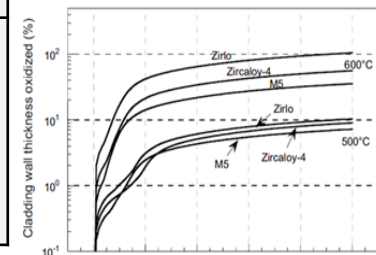
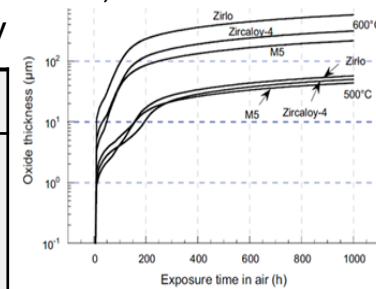
Q-14: rod cladding is M5[®] (AREVA)

The total heating power is 70 kW. About 40 % released into the inner, 60 % in the rod circuit (8 +12 fuel rod simulators, accordingly).

Test bundle surrounded by a 3.25 mm thick SH (80 mm ID) made of Zry-4 with a 37 mm thick ZrO₂ fiber insulation and an annular CJ of Inconel 600 (inner) and SS (outer tube).

Q-14 : investigation of M5[®] cladding effect on bundle oxidation and core reflood, in comparison with Q-06 where Zry-4 was used. Nearly the same protocol, to observe the effects of the change of cladding easily

Parameter	KIT_ASTEC
Zry-4/ M5 ox kinetics	Cathcart-Pawel (low temp. range)
	Prater-Courtright (high temp. range)
Cladding failure criteria (T = clad temp) (ε = ZrO ₂ layer thickness)	T > 2300 K and ε < 0.3 mm; T > 2500 K and ε > 0.3 mm



For modeling Q-14 an existing Q-06 ID, developed by S. Melis (IRSN) was adapted

- the TYPE 'SOURCE' was changed to 'BREAK', the option 'CONT 0' for imposed contact of the SH was suppressed – both thanks to a recommendation of S. Bertusi (MARCUS-cards)
- The stru for modeling convection, is subdivided to two, every of the two substructures contain only one fluid channel: CAN1 and WCAN1 **By the implemented changes, Q-14 IDs for ASTECv2.0R2p2 were obtained**

The Q-14 test phases were as follows:

Heatup to 873 K. Facility check. **Ph I** Stabilization at ~873 K. **Ph II** heat-up ~0.3-0.6 K/s to ~1500 K

Phase III Pre-ox of the test bundle in a flow of 3 g/s of superheated **steam** and 3 g/s **Ar** for ca. 3000 s at relatively const. peak temp. of ~1500 K. Withdrawal of corner rod B at the end.

Phase IV Transient heat-up with 0.3...2.0 K/s from ~1500 to ~2050 K in a flow of 3 g/s of superheated steam and 3 g/s Ar. Withdrawal of corner rod D ~30 s before quench initiation.

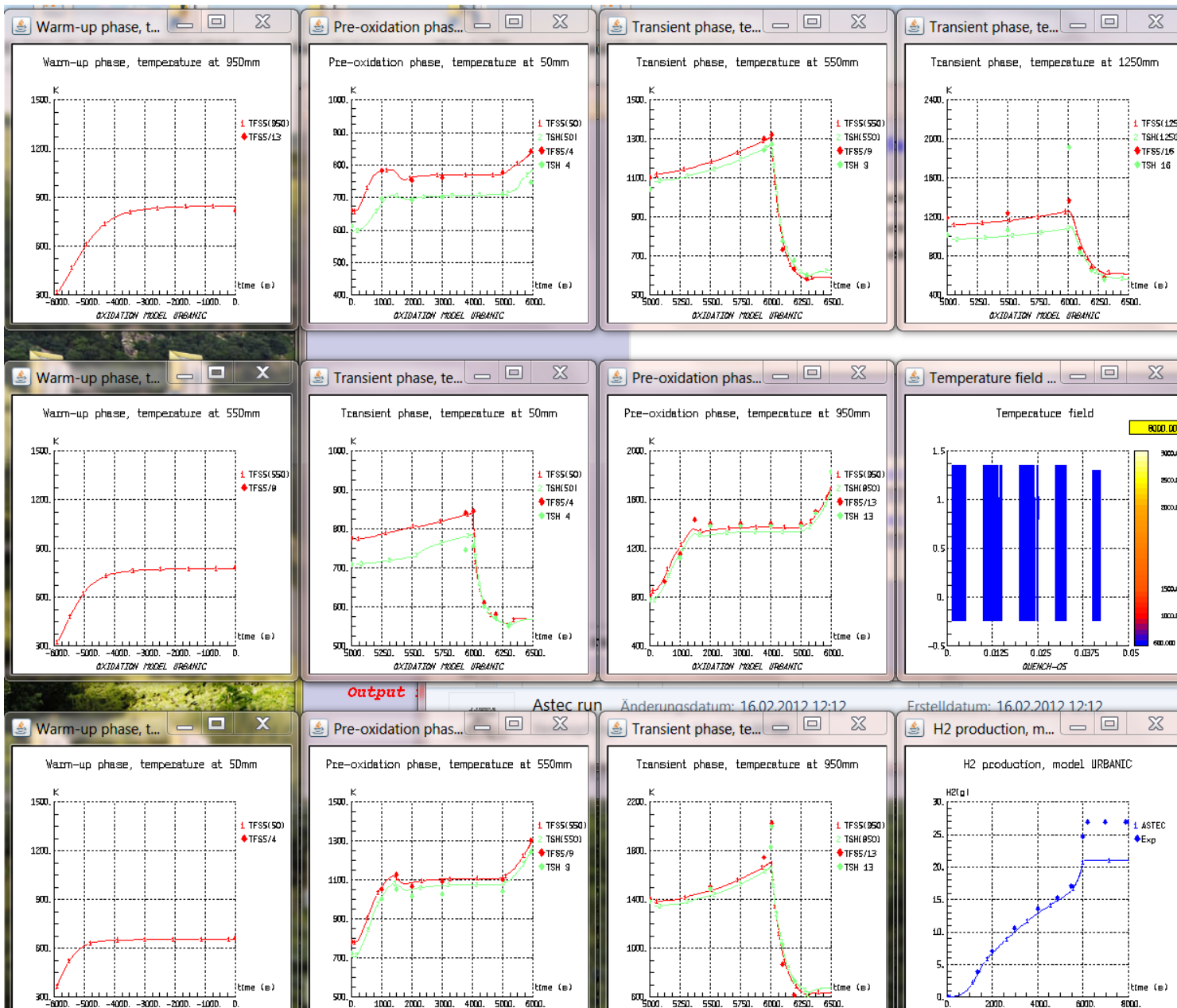
Phase V Quenching of the bundle by a flow of ~41 g/s of water.

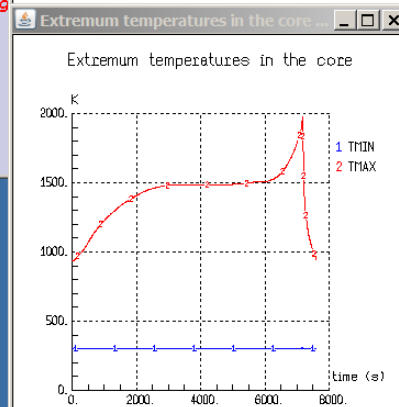
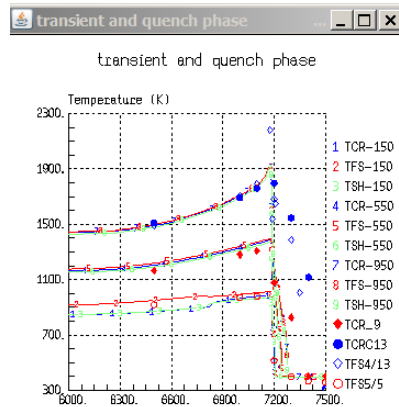
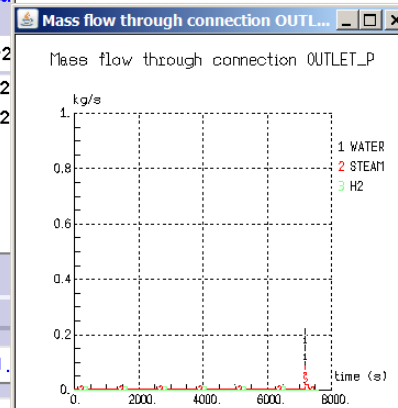
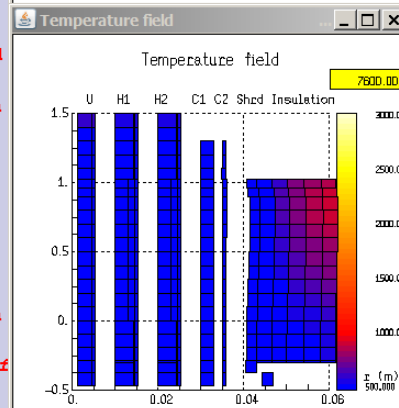
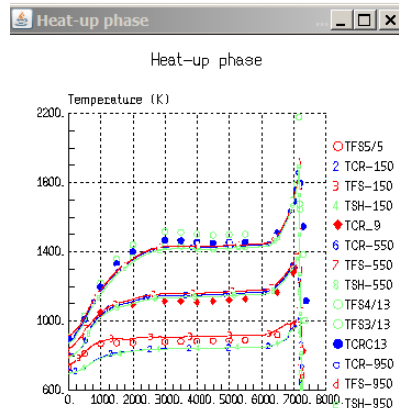
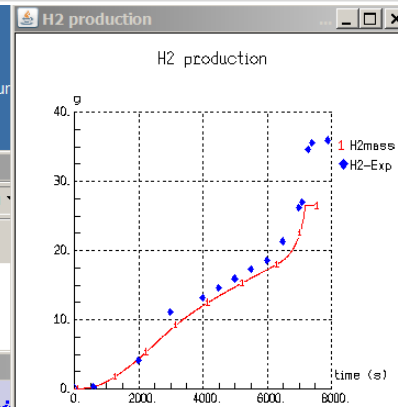
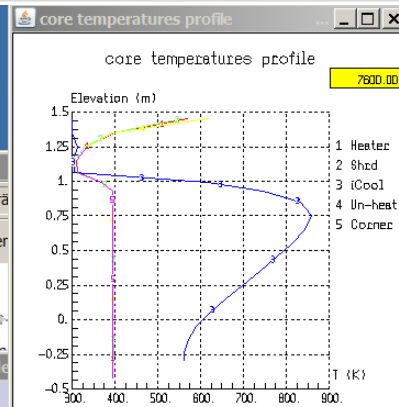
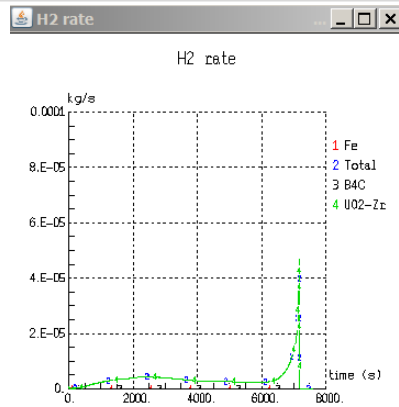
For (1073–1673)K, the M5[®] ox kinetics obtained at KIT is taken (*Mirco Grosse, SET, Fig.16*) for (1674- 2050 K) the existing data for Zry-4 were used instead of the –missing- M5[®] values

- El. power of two circuits of heating rods are changed in accordance to exp. results.
- The exp. data for temp-s are changed as they were presented for exp. data for three types of rods – central, one from the internal group and one from the outer group.
- The exp. data points for H₂ prod were changed according to exp. results from Q-6 to Q-14
- Visualization functions are added into the Q-14 ID : the rate of H₂ prod.[kg/s]; cladding layer thickness evolution vs. *t* and cladding layer thickness in function of elevation

the presented simulation for Q-14 is a proof for a lower oxidation rate of M5[®] for T<1650 K and the lower H₂ generation in the phases before quench.

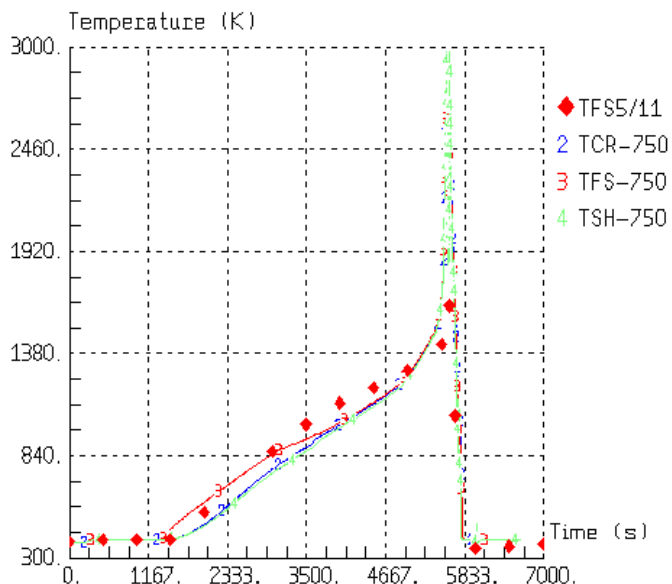
Q-05



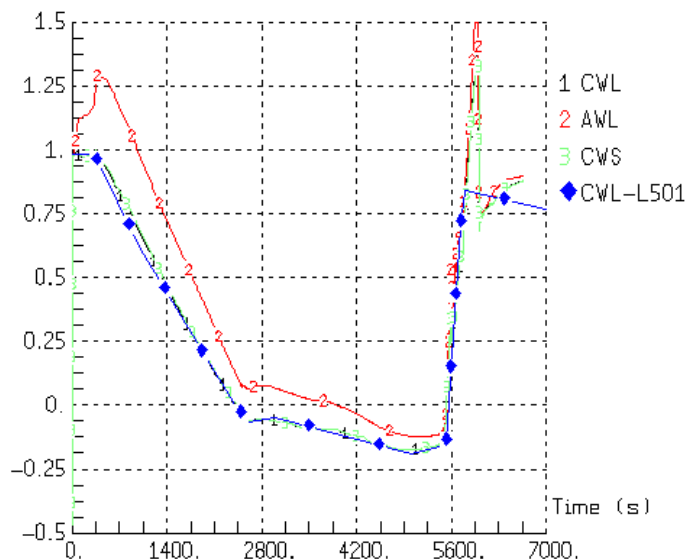


Q-06

Heat-up phase



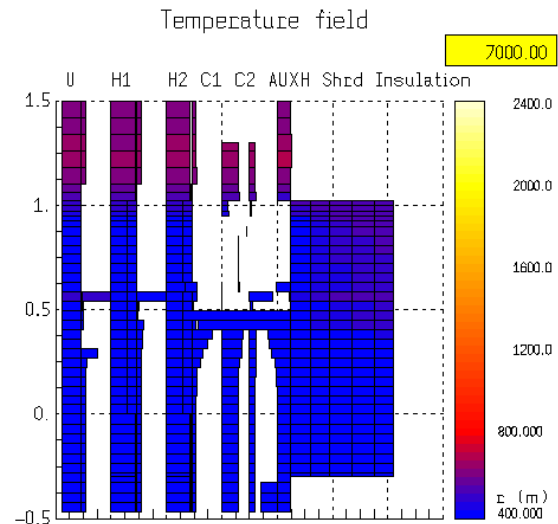
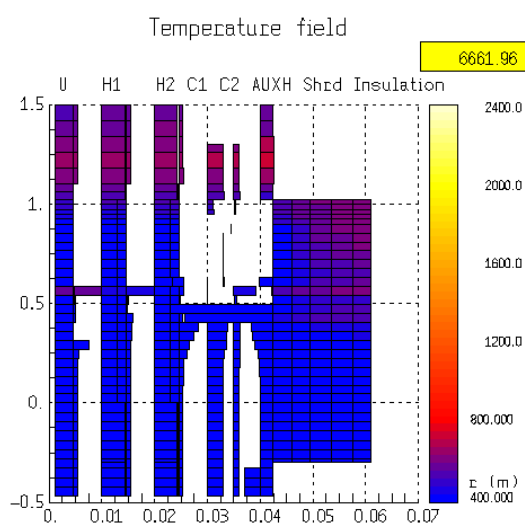
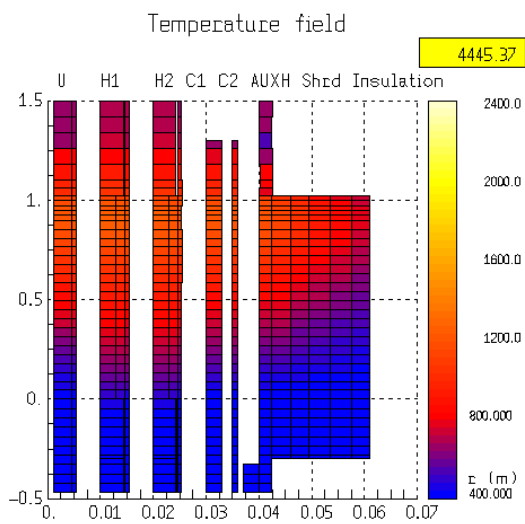
Water level (m)



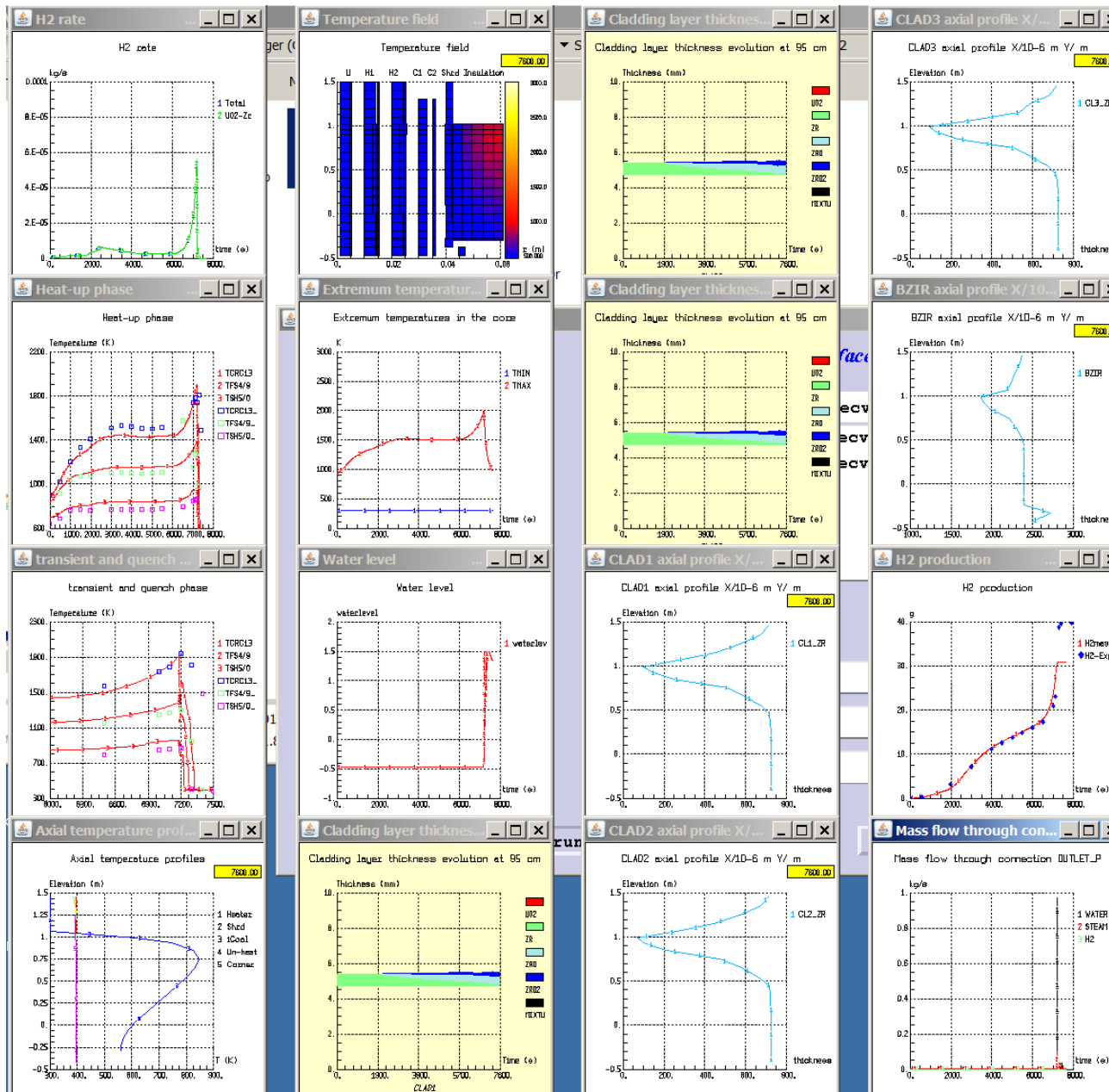
Temperature field

Temperature field

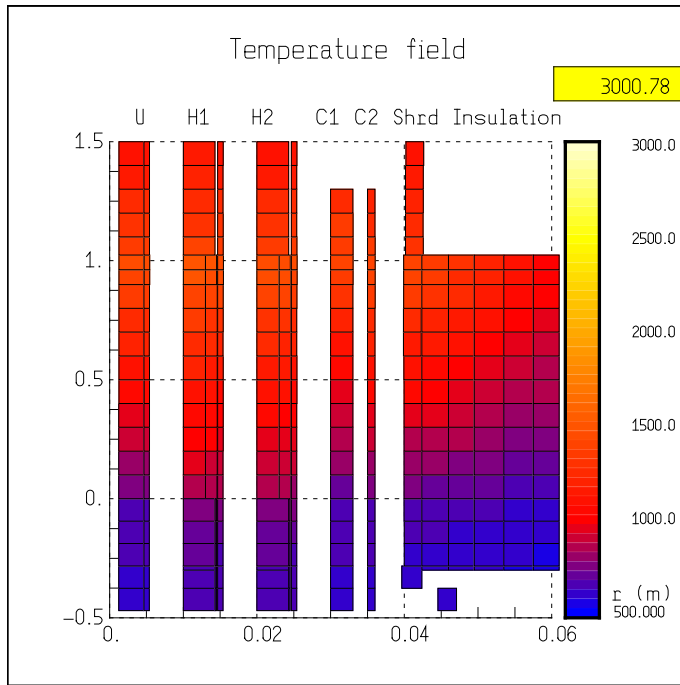
Temperature field



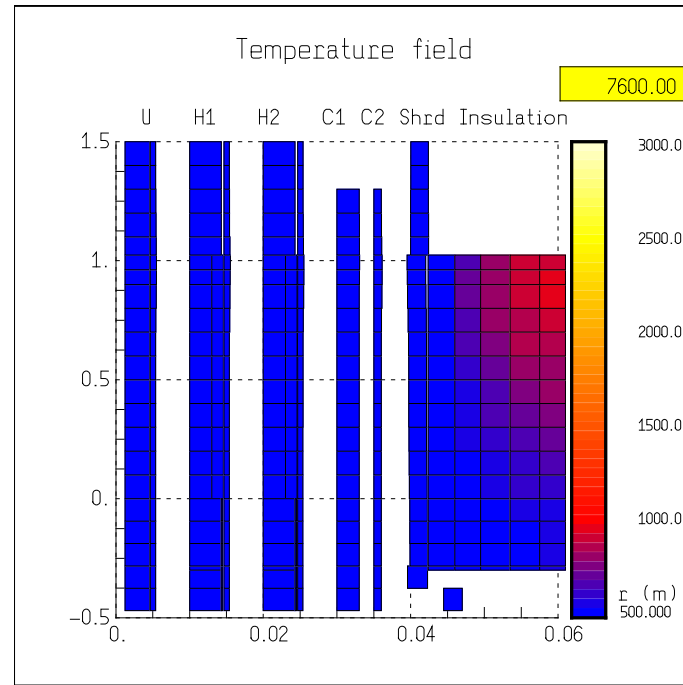
Q-14



Results using ASTECv2.0R2p2



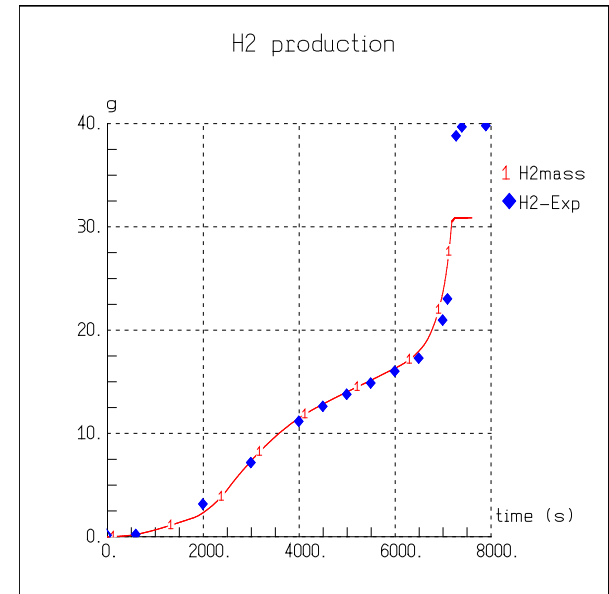
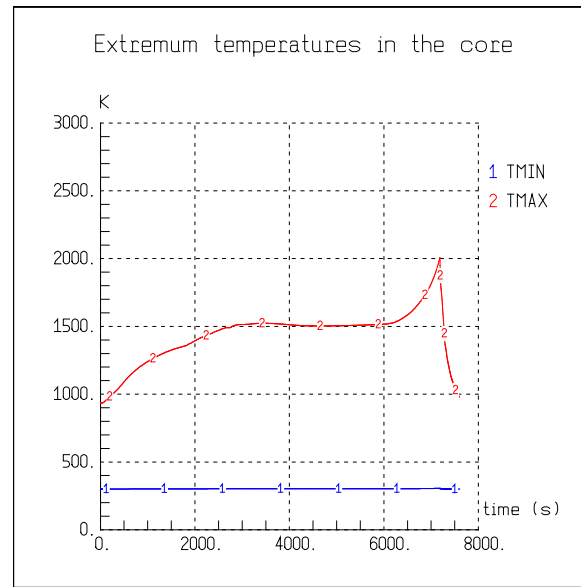
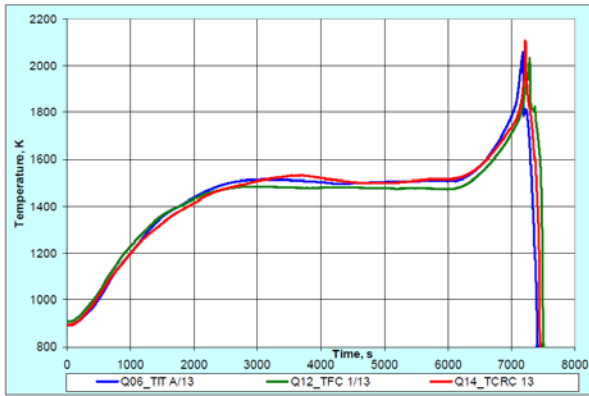
Temp. field before quenching , 3000 s



Temp. field, 7600 s – (the end)

1) central rod (U), heated rods/ inner, outer rings H1/H2, corner rods (C1;C2), SH; insulation. In the end of the calc. (7600s) the highest temp. are over the insulation and the CJ - height 750 mm

2) In correspondence to the height of max. calculated oxide thickness which was at 950 mm, Time evolution of cladding layer thickness was obtained In the end of the exp. the fraction of ZrO becomes the largest one of all. On the 2nd place the fraction of ZrO₂ and at the 3rd-the Zr contribution. In the case of inner ring rod ox. the visualization showed, that the according oxide thicknesses (ZrO and ZrO₂) are larger than in the cases of the unheated rod and outer ring rod



Maximum temp – exp. vs. ASTEC

- 1) Calc. extreme temp. (Fig. A) is close to the exp. data at “hottest” elevation of 950mm (Fig.B, but the max. calc. value just before quenching was ca 2000K in comparison to 2150 K for the exp. The difference may be explained with the ox. correlation for Zr-4 used for the highest temp-s.
- 2) The calculated H₂ prod by ASTECv2.0R2p2 is about 32g (40g in the exp). The ASTEC results are close to exp. ones in the phases before quench. at (1674-2050)K existed data for Zry-4 were used → the obtained results for H₂ prod at quench are under-estimated.

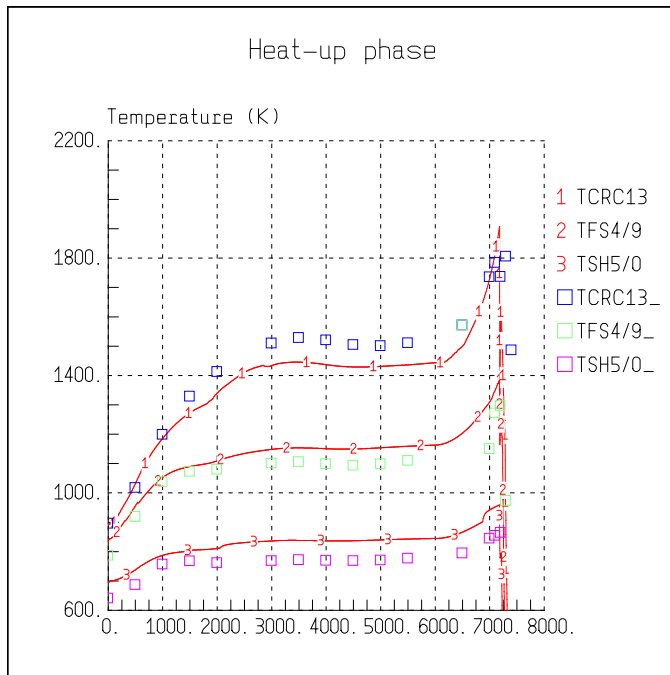


Fig.A Rod temp. – heat-up phase

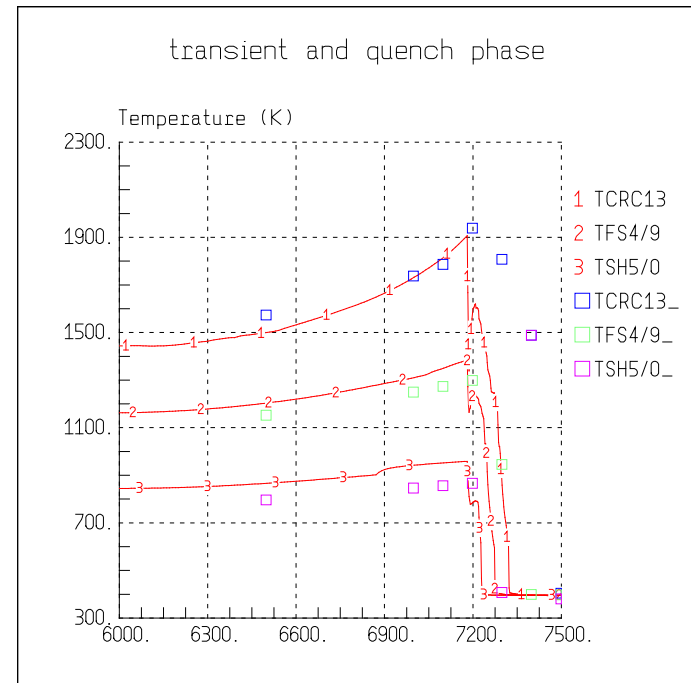
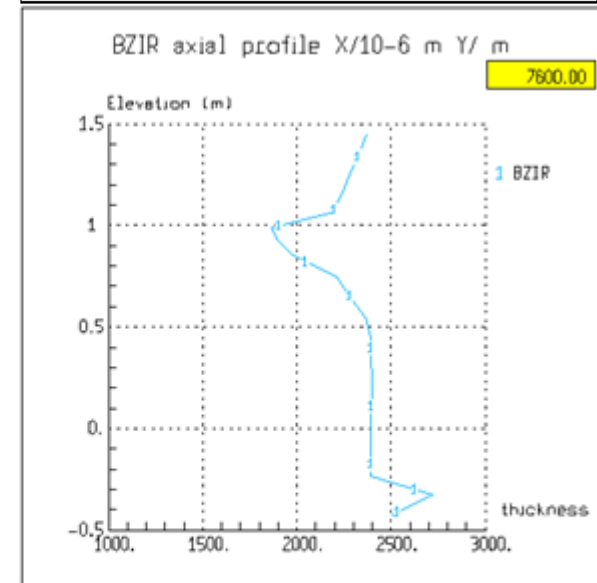
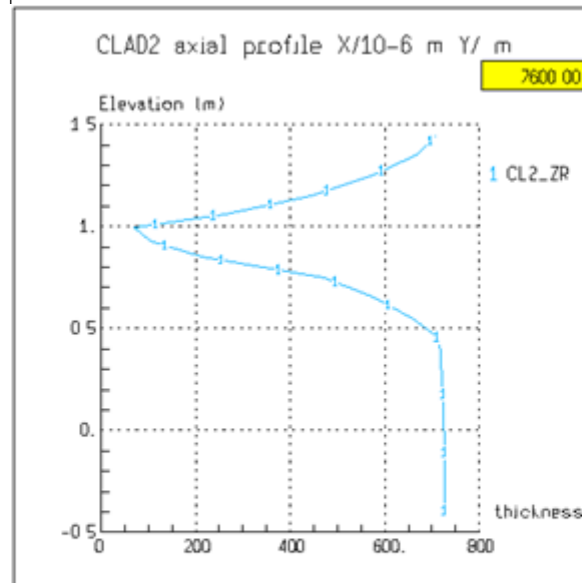
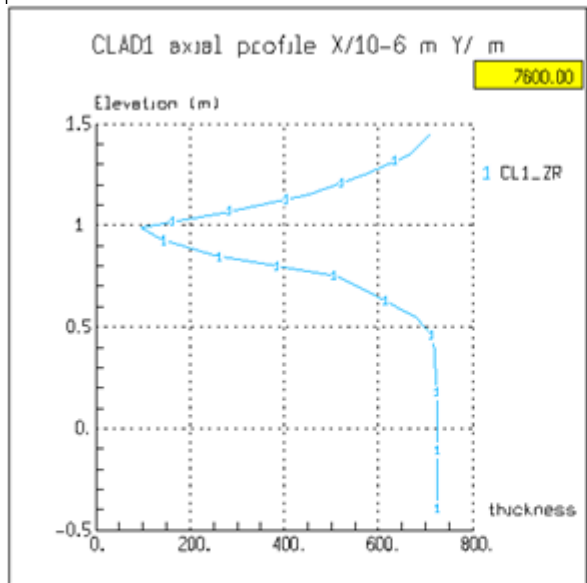
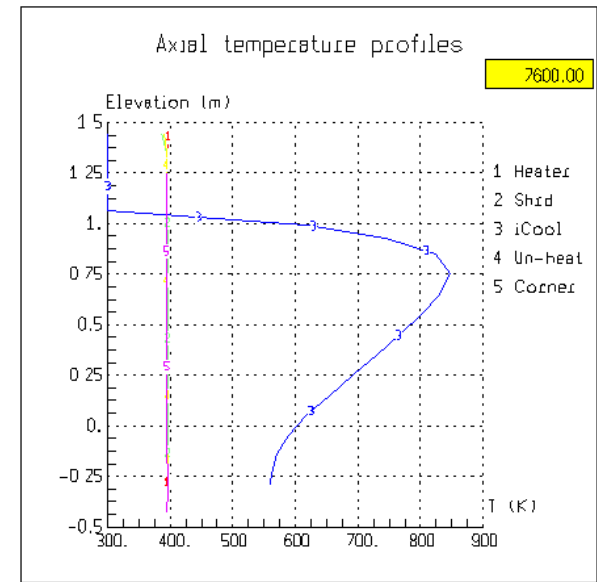
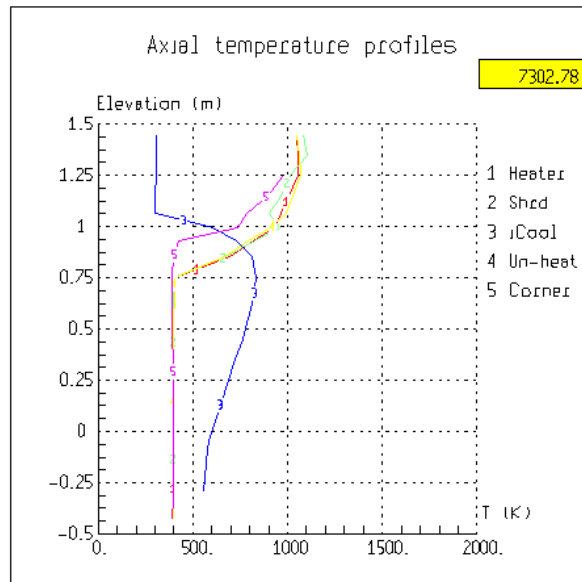
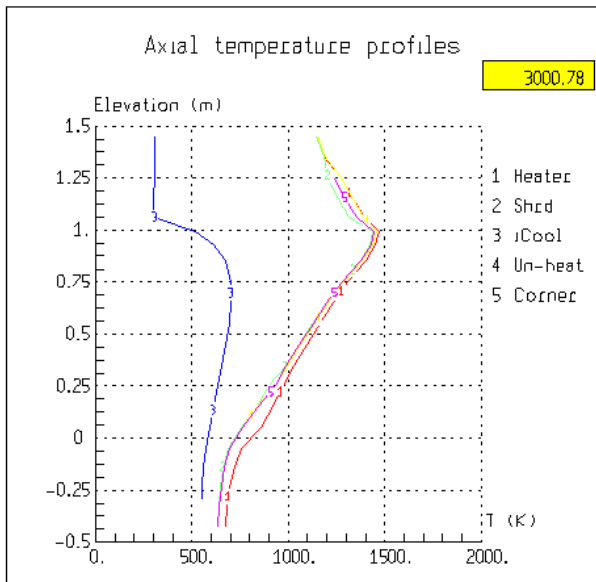


Fig.B Rod temp. – transient and quench phase

Rod temp.-s were calc: via ASTEC: unheated central fuel rod (TCRC13), one heated rod from the inner ring of 8 rods (TFS4/9) and one heated rod from the outer ring of 12 rods (TSH5/0). The highest temp.-s were calc. for the inner rod TCRC13, where the max. of ca 1900K was found just before quench. Corresponding temp. of TFS4/9 being ca 1500K and of rod TSH5/0 is 900K. There is an acceptable difference towards the exp. data of about 100K for all of the three rods.



thickness profile, 7600 s,
unheated rod

thickness profile, 7600 s,
inner ring rod

thickness profile, 7600 s,
SH

The possible reason - need for further modeling of such phenomena as

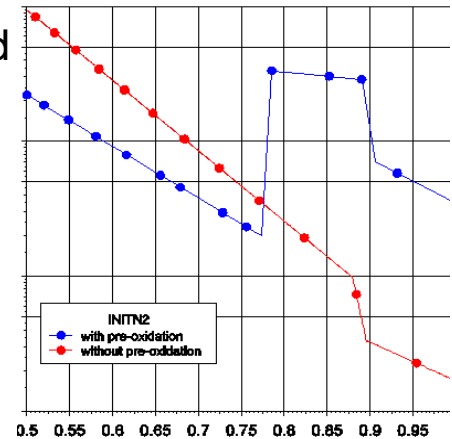
- 1) H₂ abs. and release by cladding,
- 2) oxidation of Me-melt formed between cladding and pellets;
- 3) formation of quite thick oxide layer at the inner cladding surface in the region of melt ox

The max. oxide thickness calc. for the central unheated rod is ca 630 μm at a height ca 950 mm in comparison to 860 μm at the same height from exp. At the same height, approx. the same (ca 650 μm) is the max. layer thickness for inner ring rod . For the rod from the outer ring, the max. oxide thickness is about 630 μm at the same height. In the SH calculated oxide thickness is of ca 650 μm : this result is similar to the exp. value of 590 μm.

The axial temp. profiles from the beginning of the calc. to the quench phase are similar for all rods and the SH.

and they are higher in comparison to the temp. of the CJ. The highest temp. in this time period is calc. for the heated rod in the height of about 950 mm, as in the case of the exp.

After the beginning of quench phase the temp.-s of the rods and the SH start to decrease in correspondence to rapid changes in the water level. In the end of the calc. at 7600 s, the highest temp.-s at levels down to 1 m were calc. over the CJ and the max. is found at a height around 750 mm. At heights up to 1 m the temp.-s of the rods and the SH remain higher in comparison to temp. of the CJ. (see our internal KIT-report)



- Nitride formation correlation from Th. Hollands PhD. Diss. can be used
- 2 different reaction rates with / without pre-oxidation (PO) are given;
- Reaction rate for the cases “without pre-ox” was selected up till now, as the correlation for use “with pre-ox” lead to wrong behavior (too high rates for lower temp-s; too low rates for higher temp-)
- Limitation of the calculated reaction rates to max. $2.0 \cdot 10^{-4}$ ($T > 1800$ K)
- E of activation of ZrN formation model for cases, where $p_{O_2}/p < 1.0 \cdot 10^{-2}$; full rate could be calculated if $p_{O_2}/p < 1.0 \cdot 10^{-3}$

- *The time dependency of the O_2 consumption could be calculated in good agreement with measured data with the new correlation of Steinbrück with a shift in the interpolation region*
- *The starvation condition reaches also lower bundle elevations (\rightarrow 350 mm) AIT case study: The t-dependence of the N_2 consumption can be calc. in good agreement with measured data with the correlation of Hollands (derived from SETs, Ziegler, KIT), where the rate “without pre-ox” was used;*
- *The calc. with leak simulation shows good agreement between calculated and measured liquid levels (Q- fronts)*
- *The AIT bundle is cooled down till T_{min} within 670 s after start of quenching (11350s – 12020 s) fronts / Rod temp-s during quenching (at 950 mm)*
- *Max. oxide layer of $\sim 200 \mu\text{m}$ after pre-ox (7000 s) for rods at 850 / 950 mm*
- *Max. oxide layer of $670 \mu\text{m}$ at end of simulation at 750 mm*
- *Max. **ZrN layer of $200 \mu\text{m}$** at end of simulation (15000 s) at 650 / 750 mm*

Zr-Oxo-Nitriding: process that enhances oxide degradation

- Oxide phases: ZrO_2 , ZrO_x
- Nitride phases: ZrN , Zr_3N_4
- Oxynitride phases

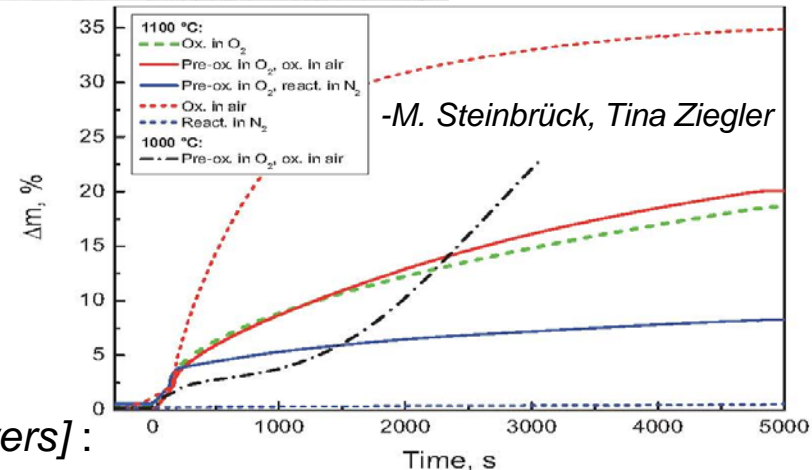
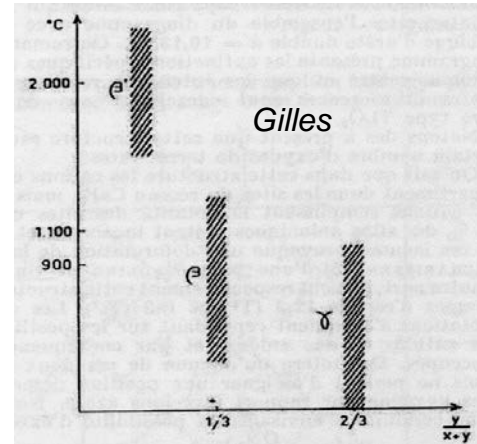
(intermediate between ZrO_2 and $ZrN_{4/3}$ i.e. $ZrO_{2-2x}N_{4x/3}$)

b': $Zr_7O_{11}N_2$: 21% mol $ZrN_{4/3}$ i.e $x = 3/14$

b: $Zr_7O_8N_4$: 43% mol $ZrN_{4/3}$ i.e $x = 3/7$

g: Zr_2ON_2 : 75% mol $ZrN_{4/3}$ i.e $x = 3/4$

Phase	$\Delta_f G$ [kJ/mol] at 2300K
ZrO_2	-675 [THERMODATA]
ZrN	-151 [THERMODATA]
$ZrON$	1071 [Gutzov]

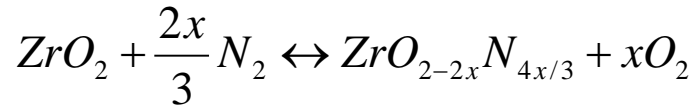


In case of simultaneous oxidation and nitriding of Zr [Powers] :

- ZrO_2 being the most stable compound; if nitriding takes place, the product will react with O_2
- Nitride will be detected only if the O_2 reaction rate becomes too slow compared with nitride rate formation...But lack of data above kinetics of O_2 reaction with nitride products

- Me creep \Rightarrow \uparrow area exposed to air/ further propagation to the whole sample
- Spatial non uniformity of the ox process \Rightarrow local init. of the breakaway transition;

It has been shown [Lerch et al.] that ZrO_2 can be nitrided directly at temp. above $1400^\circ C$ in a N_2

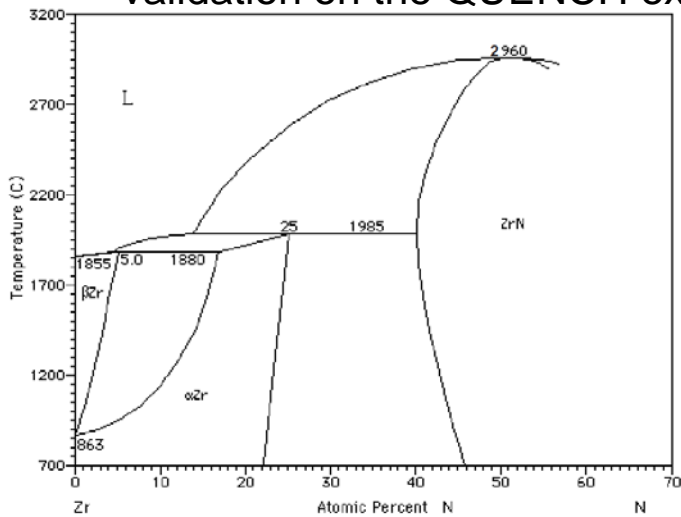


The kinetics follows a lin law, with $K_0=128$ m/s

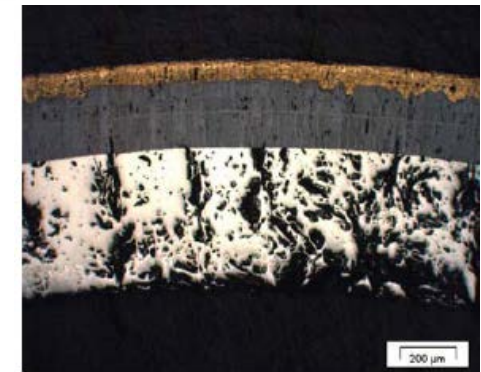
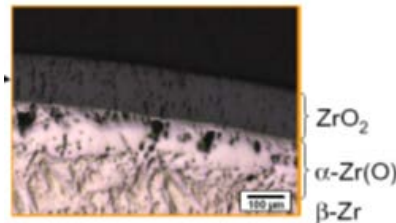
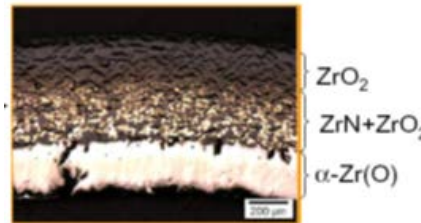
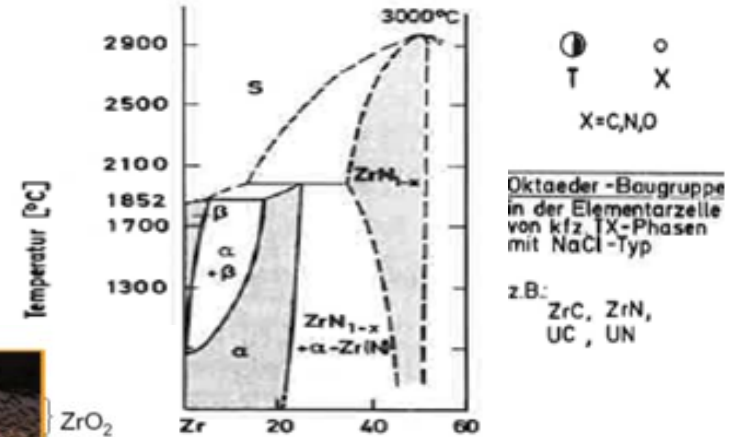
Get detailed ox kinetics data /understanding of the Zr alloys ox mechanisms



description of the air ox model in ASTEC
 ✓ validation on the QUENCH exp.-s



Phase diagram Zr-N.

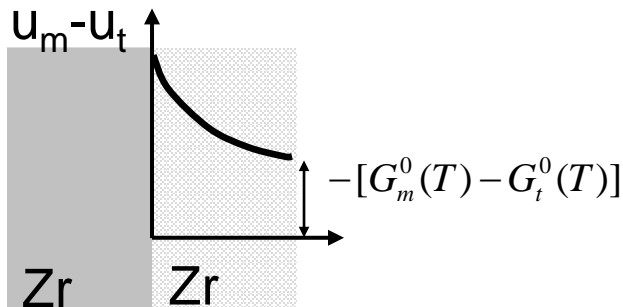


-M. Steinbrück, Tina Ziegler-

➤ some thermodynamic balance

$$\Delta G(t \rightarrow m) = \underbrace{G_m^0(T) - G_t^0(T)}_{\substack{\text{Standard free} \\ \text{energy of} \\ \text{formation}}} + \underbrace{(A_m \gamma_m - A_t \gamma_t)}_{\substack{\text{Surface} \\ \text{energy (>0)}}} + \underbrace{(u_m - u_t)}_{\substack{\text{Compressive} \\ \text{strain } E}}$$

Must be >0 to keep t-ZrO₂ stable at T < 1150°C



O₂ [Godlewski et al. 1998]

$$\Rightarrow \underbrace{u_m - u_t}_{\substack{\text{Surface} \\ \text{energy (>0)}}} > -[G_m^0(T) - G_t^0(T)] \approx -H_{tr} \left(1 - \frac{T}{T_b}\right)$$

$$f\left(\frac{1}{(\Delta m / S)}\right) = \frac{A}{(\Delta m / S)^B}$$

• ΔH_{tr} transformation of t-ZrO₂ to m-ZrO₂
T_{br}/ T_{tr} = 1150°C

➤ 1) **Correlation:** either based on the assumption that the kinetic transition is linked with transformation of tetragonal to monoclinic ZrO₂ [Cox,1976,Schanz/Leistikow 1981], or 2) Arrhenius:

$$\left(\frac{\Delta m}{S}\right)_{break} = 3.19 \times 10^5 \left(\frac{T_b}{H_{tr}(T - T_b)}\right)^{2.27328}$$

$$K = K_0 e^{-E_a / RT}$$

-Olivia Coindreau-

- we believe, that ASTEC has the potential to simulate QUENCH air ingress experiments (evidence was given here for **an other case**: Zry-4/ E110/ M5), nevertheless enthalpies of ZrN formation – still a problem; as well as nitridation as such
- **special ASTEC strength** will be the incorporation of N₂-modeling – but this not before 2014
- Dynamic behavior (time dependences; evolution)/ profiles developed can be visualized online ...
- Developing new skills / further insight into the philosophy behind ASTEC...Reference ID adopted..
- Java Data Editor **JADE/ PSPAD**: -I can recommend both here (color coding !)/ **WinMerge**, too
- captured trends must be consistent with the (intuitive) expectation
- Results are dependent on the imposed BC/IC: **Q-5/ Q-6/ Q-11; Q-14** output is satisfactory to us

- Tables, figures and spread sheets with the for **Q-10/Q-16** material will be submitted to our BE-chairwoman Leticia M., results should be presented **at the next ERMSAR 2013** meeting
- Actions foreseen for this stage: some requirements are still not fulfilled, **work is ongoing/ not completed yet, nevertheless**:
- Suggestions for the BE 1st stage followed/ (like comments to the draft , style, grammar...)
- as an outcome: **standardized Q-10/Q-16 EXCEL plots** (transients) will be delivered to PSI, and hopefully presented ERMSAR final conference
- ✓ ASTEC in SARNET2 (WP5) **Ox models at the current State of the Art/ (but not nitriding!)**
- ✓ best fit (Schanz` recommendation) kinetics of **Zry ox by steam** /sensitivity studies possible
- ✓ Coupling with **SUNSET** for uncertainty (“propagation of uncertainties”: related study): GRS, **SUSA**- approach of 1992 for “code to code” data set comparisons /final report
- ✓ Analysis of base case results regarding transient **thH** of Q-experiment plausible SA-scenarios

- Cladding Zr-4 [600-1000°C] ox kinetics can not be described only by parabolic law, because of **breakaway-transition to fast kinetics**
- Above 800°C, the transition is associated with **nitriding**. The ZrN formation begins because of a high N₂ conc. in the gas phase due to O₂ **starvation**
- Once nitriding has begun, a **porous oxide grows** under the influence of a self-sustained ZrN + O₂ → ZrO₂ + 1/2N₂ ... sequence (N₂ is trapped in the cladding). It leads to fast degradation

Air ox in pre-breakaway regime- **parabolic law**

- **Breakaway transition:** correlation between a critical weight gain at transition and temp. by an **hyperbolic law**. Assumption: breakaway transition is linked with **transformation of tetragonal to monoclinic ZrO₂**
- Post-breakaway:** modeled by an **accelerated law**, scaling rate increasing linearly

“difficulties linked to the pre-ox phase/ **limits of the models reached-it improves already the results**”

Perspectives (future prospects) further validation of the models on Q-10/ Q-16

- *in Olivia's C. AIT simulations, modeling of **the pre-breakaway by a sub-parabolic law** required*
 - *error in cladding temp prediction ⇒ K_p coeff. is strongly temp dependent*
 - *at low temp: modeling of the **post-breakaway by an accelerated law** whereas a lin kinetics observed at 850°C*
 - *Underestimation of the K_g coeff. (Arrhenius). simulated **scaling rate** is too high: 900-950°C total ox in 150-80min*
 - ***kinetic transition** occurs too early: determination of t_{break} difficult, due to the non-uniformity= inhomogeneity of the ox process (starvation conditions)*
- Olivia Coindreau-*
- *oxide layer is thicker close to air inlet, where breakaway occurs at first*

Acknowledgement: thank you, J. Stuckert, P. Kaleychev, P. Chatelard, S. Bertusi, P. Kruse, W. Hering,

Thank you all.

- ✓ further ASTEC activities: (reflood map, sensitivity..) Continuing work with **ASTEC v2.0r1p2**
- ✓ Nitradation further modeling an obvious need – preliminary / **lit. study done, also for ZrON**
- ✓ pointing out the key parameters in order to evaluate their impact on air ingress, bundle coolability and H₂ production.. (especially for **Q-10/ Q-16**) – **to be done**
- ✓ *Optional: Uncertainty Analysis* with IRSN-SUNSET or SUSA / GRS
- ✓ An ERMSAR paper will be prepared in cooperation with PSI et al.– data to be delivered soon
- ✓ Mandatory further work **still to be continued**: further developing of modified IDs exact fulfilling the BCs recommendations...)
 - early phase modeling (HT, mechanical behavior, chemistry, movement of material)
 - the instantaneous or t cumulated (integral) H₂ production rate [kg/s]/ [kg] during the Q- phase

OC- Lit: study: CITATION “temp rises too quickly during the air ingress in the simulations:

- Protective oxide layer not thick enough,
- T correlations used up till now (for **non PO** cladding) overestimate the mass gain (and so the enthalpy of the chemical reaction) for **PO cladding**

Not enough N₂ taken from the gas phase:

Criterion to switch from ox. to nitridation based on an inappropriate “critical starvation coeff.”

Not enough H₂ generated during reflood:

- Specific models for reflood and **shattering** should be used including **ox. after nitridation**

Lacks in ICARE modeling identified, consulted with P. Chatelard (**development currently underway: ASTEC source code changes to be finished 2014 as a part of ASTEC v2.1– info IRSN**):

suitable criterion to switch from ox to nitradation (probable influence of the th-Hydraulics)

- model for **reox of ZrN for scale** thicknesses at the end of the pre-ox phase, where reox. is quite low”